Int J Thermophys (2007) 28:968–979
DOI 10.1007/s10765-007-0215-x

Development of Nanoscale Temperature Measurement Technique Using Near-field Fluorescence

T. Jigami · M. Kobayashi · Y. Taguchi · Y. Nagasaka

Published online: 21 August 2007

Abstract A nanoscale thermal system design, especially for the precise measurement of the temperature distribution in microfabricated devices using novel nanomaterials such as carbon nanotubes and fullerene has become increasingly important along with the development of nanotechnology. A new approach has been proposed toward an optical nanoscale temperature measurement method using near-field optics and fluorescence thermometry, namely, Fluor-NOTN (fluorescent near-field optics thermal nanoscopy). The topographic image and temperature dependence of a fluorescently modified sample, excited by near-field light, are simultaneously monitored. In this article, the temperature dependence of Cy3 fluorescent dye is verified near room temperature (298–308 K). A Cy3 mono-dispersed sample of a permalloy ($Ni_{81}Fe_{19}$) wire heater, 500 nm in width and 100 nm in thickness, is designed and fabricated. A localized temperature gradient of $\Delta T = 4$ K within a submicron distance from the heater was successfully detected by near-field fluorescence with 100 nm spatial resolution.

Keywords Fluorescence · Nanoscale · Near-field light · Spatial resolution · Thermometry

T. Jigami · M. Kobayashi
School of Integrated Design Engineering, Keio University, 3-14-1, Hiyoshi, Yokohama, Kanagawa 223-8522, Japan

Y. Taguchi (✉) · Y. Nagasaka
Department of System Design Engineering, Keio University, 3-14-1, Hiyoshi, Yokohama, Kanagawa 223-8522, Japan
e-mail: tag@sd.keio.ac.jp

1 Introduction

As nanotechnology advances and expands its applications over a broad area, thermal measurements at the nanoscale have become increasingly important. A thermal device design scaled below the micrometer level has already been devised using novel nano-materials such as carbon nanotubes and fullerenes [1,2]. For example, a carbon nanotube has an exceptional ability for electron transport and thermal conduction, which represents a promising material for future electronic devices. However, due to characteristic phenomena at the mesoscopic scale, where the representative length is comparable to the mean free path of the material, various size effects such as ballistic electron transport may yield a difference in the heat transfer mechanism [3,4]. The complication of thermal analysis is a barrier to optimal thermal design of nanoscale devices, and therefore, measurements of temperature for both local heat generation detection and elucidation of heat transfer phenomena at the mesoscopic scale are strongly needed.

There have been several different techniques developed for microscopic thermometry that target on nanostructures. However, among them, there are cases where the spatial resolution is limited to the micrometer level or the method itself still remains qualitative. A contact method such as scanning thermal microscopy is often represented by problems of the unverified mechanism of heat transfer between the probe tip and the sample [5]. As for a carbon nano-thermometer, it has not been applied to actual temperature measurements, because carbon nanotube handling has not yet been established. Also, the result of the measurement must be observed using a scanning electron microscope [6]. The spatial resolution of microchannel fluorescence imaging remains above the micrometer level due to the diffraction limit of light [7,8]. From the above reasons, it can be stated that these techniques are unable to meet the need.

As a non-contact and non-destructive temperature measurement technique possessing high-spatial resolution, we introduce a novel approach, namely Fluor-NOTN (fluorescence near-field optics thermal nanoscopy), which utilizes fluorescence near-field light [9]. Near-field light excites fluorescent probes modified onto the sample substrate. The detected fluorescent intensity contains information on the sample temperature from its temperature dependence. The use of near-field fluorescence enables local temperature measurement under high spatial resolution on the nanometer level, surpassing the diffraction limit of light. Samples can be selected from any material, both solids and liquids, which can be modified molecularly with fluorescent probes. Moreover, the temperature range and resolution can be adjusted by selecting the proper probe. As a candidate fluorphore, fullerene can be selected for nanoscale temperature measurements. There have been reports that a fullerene indicates the temperature dependence of fluorescence [10,11]. Therefore, with the combination of near-field optics and a fullerene as a fluorescent probe for temperature measurement, it is possible to reach a spatial resolution as small as 10 nm, which is set as the final goal of Fluor-NOTN.

In this article, the following results are reported: (a) the fluorescent spectrum and temperature dependence of Cy3 fluorescent dye was measured, (b) as a test sample for nanoscale temperature measurements, a wire heater, 500 nm in width, was fabricated, (c) a near-field scan of heater surface topography and fluorescent distribution

surrounding the nanoscale wire heater was conducted, and (d) a localized temperature gradient was detected within a submicron distance from the wire heater.

2 Measurement Theory

2.1 Near-field Optics

In order to surpass the diffraction limit of light, Fluor-NOTN utilizes near-field light for measurement, as shown in Fig. 1. Near-field light is generated at the tip of a near-field optical fiber for which its aperture diameter is much smaller than the wavelength of the irradiated light. At the tip of the near-field optical fiber, an electric field $\mathbf{E}_0$ is applied by the incident laser. The electrical dipole moment that interacts between the fiber and the sample induces the polarizability variation. When the distance between the two is r, the polarizability variation $\Delta\psi$ can be expressed as

$$\Delta\psi = \frac{\psi_\mathrm{p}\psi_\mathrm{s}}{2\pi\varepsilon_0 r^3}, \tag{1}$$

where ψ_p and ψ_s are polarizability variations of the fiber and the sample, respectively, and ε_0 is the dielectric constant. Thus, the intensity of the scattered light I_s from the sample is expressed as [12]

$$\begin{aligned} I_\mathrm{s} &\propto \left|\left(\psi_\mathrm{p}\mathbf{E}_0 + \Delta\psi\mathbf{E}_0\right) + \left(\psi_\mathrm{s}\mathbf{E}_0 + \Delta\psi\mathbf{E}_0\right)\right|^2 \\ &\approx \left(\psi_\mathrm{p} + \psi_\mathrm{s}\right)^2 |\mathbf{E}_0|^2 + 4\Delta\psi\left(\psi_\mathrm{p} + \psi_\mathrm{s}\right)|\mathbf{E}_0|^2 . \end{aligned} \tag{2}$$

In the above function, the term that includes $\Delta\psi^2$ is regarded as negligible. The first term in Eq. 2 represents the propagation light element, which overlaps onto the signal as background noise. The second term represents the scattered light element of the near-field light, and it indicates that the intensity of the near-field light attenuates exponentially with the distance away from the fiber tip. Since the size of the near-field light depends merely on the aperture of the fiber and not on the wavelength of the incident light, Fluor-NOTN enables optical temperature measurements for nanoscale spatial resolution beyond the diffraction limit of light.

2.2 Temperature Dependence of Fluorescence Intensity

Flour-NOTN utilizes the temperature dependence of a fluorophore for thermometry and, therefore, the objective sample must be modified fluorescently. In fluorescence emission, electrons from the excited state transit to the ground state in two paths, radiative process and non-radiative process. A fluorescence quantum yield φ is expressed theoretically as

$$\varphi = \frac{W_\mathrm{R}}{W_\mathrm{R} + W_\mathrm{NR}}, \tag{3}$$

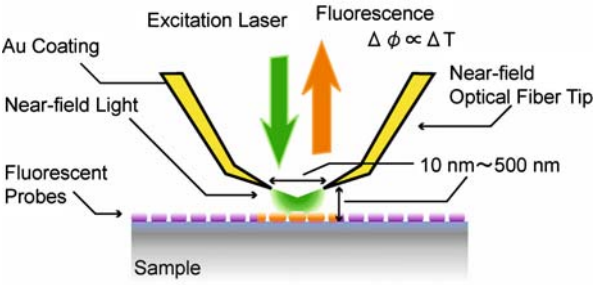

Fig. 1 Schematic image of Fluor-NOTN. Excitation laser is irradiated into near-field optical fiber, generating near-field light at the fiber tip. Fluorescent probes that are modified onto the sample emit fluorescence as returning light into the fiber. The fluorescence intensity is temperature dependent

where W_R is the rate constant for radiative deactivation and W_{NR} is for non-radiative deactivation. W_{NR} can be expressed as [13]

$$W_{NR} = s \exp \frac{-\Delta U}{k_B T}, \tag{4}$$

where s is the frequency factor, ΔU is the thermal energy of activation, T is the temperature, and k_B is the Boltzmann constant. As the temperature increases, the non-radiative process becomes dominant, indicating a decrease in the fluorescent intensity. This is called temperature quenching of the fluorophores. Thermal agitation such as the phonon vibration is exemplary among non-radiative processes. The rate of quenching and the temperature range vary according to the types of flourophores.

3 Experimental Apparatus

A schematic image of the experimental apparatus of Fluor-NOTN is illustrated in Fig. 2. An excitation laser (Nd: YAG, wavelength of 532 nm) is coupled into the near-field optical fiber via mirrors, a beam splitter, and wave plates. The excitation laser generates near-field light at the tip of the fiber, which then excites fluorophores modified on the sample. Fluorescence is collected by the same fiber, and outputs from the fiber coupler into the photomultiplier tube (PMT) via a beam splitter. A high-pass filter is placed in front of the detector in order to cut off unnecessary signals, such as reflected light from the fiber tip, the coupler, and the wave plates.

The fiber is attached to a quartz crystal tuning fork, in order to actuate precise distance control at the nanoscale. The fiber is vibrated at its resonant frequency, and the change of resonance can be detected due to the shear force (e.g., Van der Waals force) as the fiber approaches the sample. Monitoring of the resonance frequency enables distance control of the fiber probe and the sample as well as topographic scanning of the sample surface.

A near-field optical fiber is vibrated at a constant frequency in the vertical direction for the purpose of extracting the weak fluorescence signal with high sensitivity. As explained previously, the intensity of the near-field light decays exponentially from

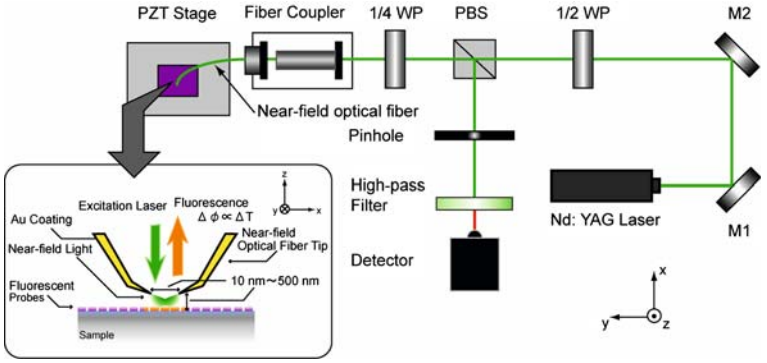

Fig. 2 Experimental apparatus of Fluor-NOTN. Excitation laser is coupled into near-field optical fiber via mirrors (M), wave plates (WP), and a polarized beam splitter (PBS). Near-field light is generated at the tip of the fiber, which is adhered to a quartz crystal tuning fork. As the fiber approaches in a vertical direction toward the sample substrate, the vibration amplitude decay, due to the shift of the resonant frequency caused by a shear force, is monitored and kept constant with a PID feedback controller. The fluorescence signal collected by the fiber is reflected at the beam splitter into the detector

the tip of the aperture in the vertical direction. By modulating the fiber-sample distance periodically and utilizing electrical band-pass filtering, the target signal can be extracted with a high signal-to-noise ratio.

As the fiber probe scans in the horizontal direction over the sample surface, the fluorescence intensity and vertical displacement of the fiber can be determined simultaneously with the photomultiplier tube and digital oscilloscope, respectively. Thus, Fluor-NOTN is able to acquire both two-dimensional topographic images and the surface temperature distribution of the sample.

4 Sample Preparation

For a quantitative comparison of measurements and theoretical calculations, the scanned sample must be simply structured to be able to calculate its temperature profile. In order to satisfy the requirement, we have designed and fabricated a sample metallic wire heater of 500 nm in width and 100 nm in thickness. The purpose of fabricating a sample heater is to evaluate the spatial and temperature resolution of Fluor-NOTN.

4.1 Theoretical Calculation of Temperature Distribution

A sample heater is required to generate a temperature gradient within a submicron region for nanoscale temperature measurements. For optimal design of the dimensions of a wire heater, we carried out a two-dimensional heat conduction calculation using the finite difference method. Figure 3 (inset) shows a schematic image of the boundary conditions set for the simulation. For optimal heater design, a temperature increase of 5 K or higher under 10 mA of current applied to the heater was required.

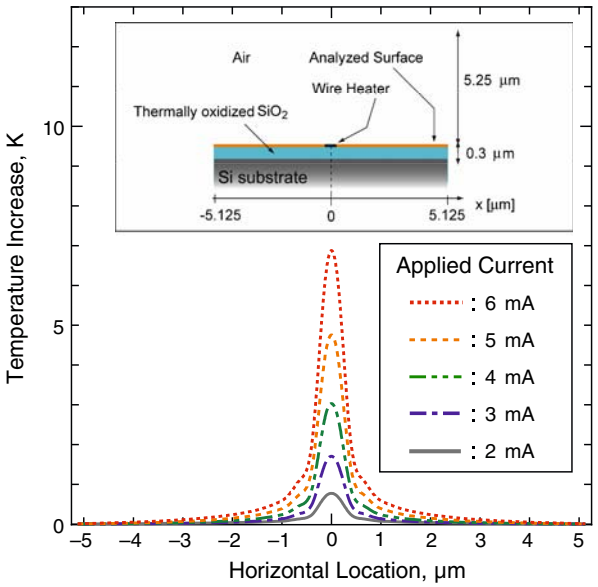

Fig. 3 Calculated results of temperature distribution created around the wire heater sample. 6 mA of current applied to the heater is estimated to create 6 K gradient within a submicron region. The schematic image of boundary conditions for simulation of temperature distribution is shown at top left. The wire heater sample is placed on thermally oxidized SiO_2 layer over the silicon substrate. Analyzed area covers 5.28 μm in height and 10.25 μm in width

Therefore, the proper selection of a wire material with adequate electrical resistivity for Joule heating was essential.

A metallic heater is placed on a silicon substrate with a thin membrane (nominal thickness: 100–200 nm) of silicon dioxide on its surface. Parameters used for calculations are the thermal conductivity, electrical resistivity, and applied current [14]. Figure 3 shows the calculated results of the temperature distribution surrounding the wire heater for different amounts of applied current. For an adequate electrical resistivity value for Joule heating, we have selected permalloy ($Ni_{81}Fe_{19}$) as the heater material.

A steep temperature gradient within a submicron region generated by the wire heater is shown in Fig. 3. Temperature differences with a maximum of 6 K can be observed by controlling the applied current up to 6 mA. The numerical simulation indicates that a permalloy wire of 500 nm in thickness is suitable for the nanoscale temperature measurement test sample as well as for evaluating both spatial and temperature resolutions.

In fact, the thermal conductivity may be lower and the electrical resistivity may be higher than the bulk value because permalloy was layered by physical vapor deposition, creating a polycrystalline structure, which scatters electrons/phonons at the grain boundary. However, it can be considered that the relative temperature measurements, as were carried out in this article, and the simulation results are adequately comparable.

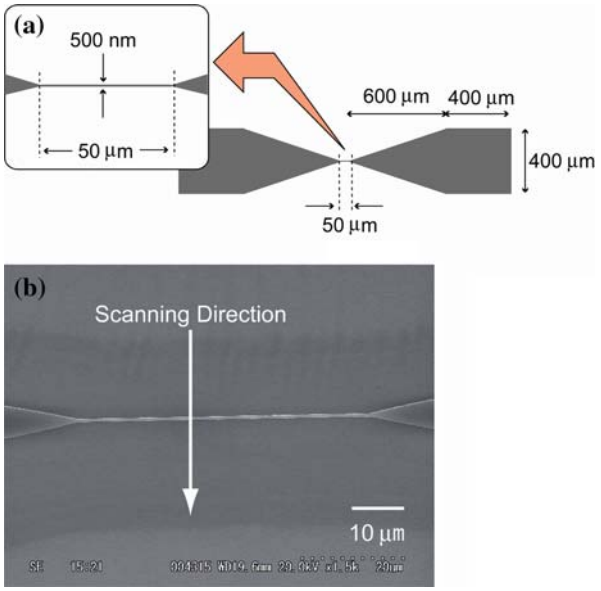

Fig. 4 (**a**) Schematic image of the wire heater sample. A 50 μm length wire heater is wedged between electrodes (1 mm in width and 400 μm in height). The shape of the electrodes is designed to avoid disconnection of wire due to electro-current constriction. (**b**) SEM (scanning electron microscope) image of the wire-heater sample. The width of the wire heater is measured to be approximately 500 nm, and its length is 50 μm. A firm connection of wire to the electrodes is confirmed. The scanning direction of the near-field optical fiber, perpendicular to the wire heater, is shown with white arrow

4.2 Fabrication of Wire-heater Sample

Based on the results from the simulation, we have fabricated a wire heater, 500 nm in width, using electron beam resist patterning. Figure 4a shows a schematic image of the wire heater, with a length of 50 μm which is wedged between a pair of electrodes. The electrodes are triangularly shaped in order to avoid disconnection of the wire due to electro-current constriction.

In the process of fabrication, a 150 nm thick electron beam sensitive resist was first spin-coated onto a thermally oxidized SiO_2 layer on a silicon substrate. The shape of the heater and the electrodes was drawn over the resist by an electron beam and the irradiated part was removed. Permalloy was then layered above the resist by physical vapor deposition, and the wire heater was patterned by the liftoff. The precise size of the wire heater was measured with an SEM image (Fig. 4b) and AFM, width of 500 nm and height of 100 nm. Uniform fabrication of the wire heater was successful.

5 Results and Discussion

5.1 Temperature Dependence of Cy3 Fluorescent Dye

For selection of the fluorescent probe, there were several conditions to be satisfied: (a) fluorophore with a large temperature dependence, (b) fluorophore with high

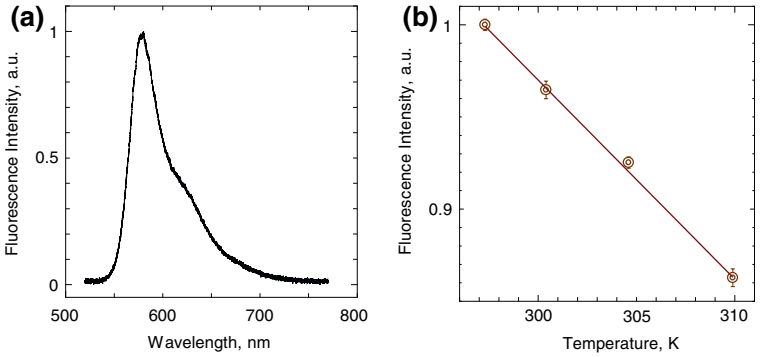

Fig. 5 (**a**) Fluorescence spectrum of mono-dispersed Cy3 dye on SiO_2 layer on a silicon substrate, measured with a fluorescent microscope. Excitation wavelength is 514.5 nm with Ar^+ laser. Fluorescent emission maximum is at a wavelength of 580 nm. (**b**) Temperature dependence of fluorescent intensity detected using fluorescent microscope. Temperature ranged from 298 K to 308 K. Temperature coefficient is calculated as $0.01\,K^{-1}$

extinction coefficient and quantum yield, (c) unequivocal fluorescent emission wavelength that does not overlap with autofluorescence of the sample, (d) fluorophore with stable fluorescent intensity without much bleaching, and (e) fluorophore modifiability as a uniform mono-layer onto a dry SiO_2 surface. Based on the above criteria, mono-reactive NHS ester Cy3 dye was selected.

Cy3 dye is commonly used as a fluorescent probe for micro-array genomics analysis, DNA, cells, proteins, and antibodies for its stability [15–17]. Other than to elucidate the mutual effect of protein and DNA, the temperature dependence of Cy3 enables the observation and measurement of molecular thermodynamics during chemical reactions. For the fabricated sample, Cy3 must be bonded onto a dry substrate. However, the measurement of temperature using dried Cy3 dye is unprecedented, and, therefore, the temperature dependence of mono-layered Cy3 on a dry sample substrate was unknown.

As a preliminary measurement for the property evaluation of Cy3 in a dried state, the fluorescent spectrum and temperature dependence of the Cy3 dye modified onto the glass substrate was measured using a fluorescent microscope (Fig. 5). Mono-dispersed Cy3 dye molecules, covalently attached on a glass surface via the amino group, were excited with an Ar^+ laser (wavelength of 514.5 nm) focused by an objective lens in the fluorescent microscope. The glass substrate was heated by a Peltier device from room temperature to 308 K.

Figure 5a indicates the fluorescent emission spectrum of Cy3 dye on a glass plate. The peak wavelength of fluorescence was measured to be approximately 580 nm. Ordinarily, the emission maximum of Cy3 dye dissolved in a dimethyl sulfoxide aqueous solution is 561 nm. Approximately 20 nm difference was confirmed due to the difference in molecular interaction of measured states, i.e., between a dried mono-layered state and one dissolved in solution.

In Fig. 5b, an inverse relationship between the fluorescent intensity and temperature is shown. Also, the glass substrate was cooled to room temperature after the

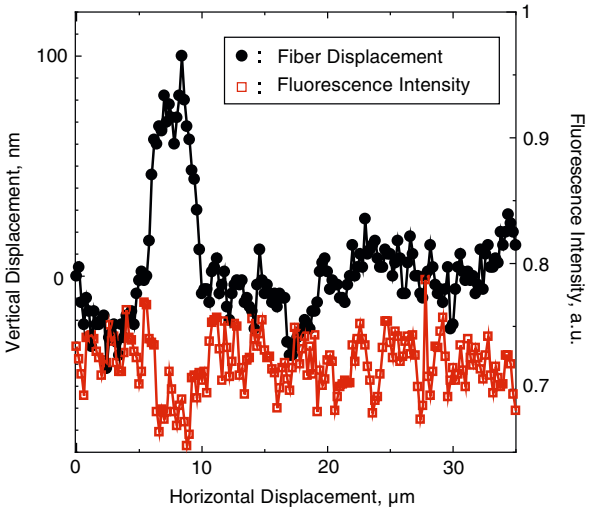

Fig. 6 Scanned surface topography and fluorescent distribution of sample surface. Circles indicate vertical displacement of fiber, and squares indicate localized fluorescent intensity

measurement. The fluorescent intensity detected prior to and after heating showed similar values. Therefore, Fig. 5b indicates excellent reversibility and repeatability near room temperature, validating the use of Cy3 as a fluorescent probe for temperature measurement. The temperature coefficient was calculated as $0.01\,K^{-1}$.

5.2 Topography and Fluorescent Distribution of Heater Sample

The performance of the positioning and the detection system of Fluor-NOTN was verified prior to the temperature measurement of the sample heater. The surface topography and fluorescent intensity distribution were simultaneously scanned using a near-field optical fiber in the direction shown in Fig. 4.

In Fig. 6, the vertical displacement of the fiber located the wire heater 8–10 μm from the scan starting point. The fluorescent intensity decreases above the heater because Cy3 molecules covalently bond only over the SiO_2 surface, and not over the permalloy surface. The full width at half maximum of the vertical fiber displacement in Fig. 6 was approximately 1.8 μm which is much wider than the actual 500 nm dimension of the heater. The result engulfs the double width of the fiber tip diameter (at the front and back of the wire heater) while scanning. The total scanning time for the measurement shown in Fig. 6 was approximately 30 min, plotting 350 points under 5 s each. Although the distance control between the fiber tip and the sample is considered stabilized in less than 5 s, it may take a longer period of time over the wire heater surface, increasing the background noise. Also, the background noise is possibly caused by the broad-based fluorescence from the fiber core (Ge-doped SiO_2) of which its wavelength is near 580 nm.

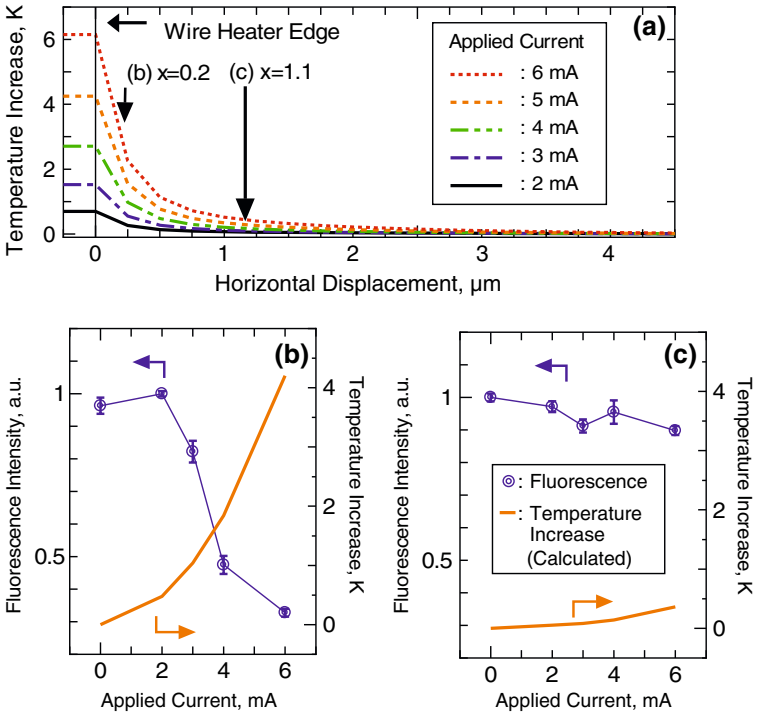

Fig. 7 (**a**) Calculated temperature increases at each point, with applied current ranging from 2 mA to 6 mA, are indicated with various dotted lines. Simulation results show that the temperature gradient is created between points at distances of 0.2 and 1.1 μm from the heater edge (the point of origin). (**b**) Fluorescent intensity decreases drastically at 0.2 μm away from the heater edge, indicating the significant localized temperature rise. (**c**) Signal detected at 1.1 μm from the heater edge indicates little decrease in intensity, indicating small temperature rise

The results indicate the ability to detect the 100 nm thickness of the wire heater and the difference of the near-field fluorescence intensity for modified and unmodified material surfaces.

5.3 Detection of Localized Temperature Gradient

From the simulation result shown in Fig. 3, a temperature difference of approximately 4 K is calculated to be generated within a submicron region. The temperature change of two spots, 900 nm apart, was detected as the fluorescent intensity decay, both spots within 1 μm distance from the heater edge (Fig. 7a). The fluorescent intensity decay at two localized points is compared in Fig. 7b, c.

Figure 7b, c compares the relative difference of the fluorescence intensity decrease at two points. The fluorescence intensity at $x = 0.2\,\mu$m shows greater quenching indicating a greater temperature increase, whereas the fluorescent intensity at $x = 1.1\,\mu$m show little quenching. The difference in quenching of the two measured points

indicates that the temperature gradient generated by the heater has been detected in a submicron region using 100 nm apertured near-field light.

The fluorescence intensity level from the temperature calibration in Fig. 5b appears significantly different from those shown in Fig. 7b, c. The most dominant cause of the difference in calibration is considered to be the photobleaching effect of Cy3 dye. In this measurement, the fiber probe was set within the near-field distance for over 60 s for obtaining each plot. Therefore, the photobleaching effect of the Cy3 molecules could have accelerated the fluorescence intensity decay. The required time for measurement was approximately 60 s for each plot, which is required for steady-state heating of the wire heater. The photobleaching effect possibly occurred during the waiting time.

The temperature resolution of Fluor-NOTN is yet to be defined. However, the result (Fig. 7b, c) indicates successful detection of a localized temperature gradient of approximately 4 K using near-field light. Further study on improving the signal-to-noise ratio, the stability of the sample-fiber distance, and the repeatability would achieve quantitative evaluation of the temperature resolution using near-field light. This indicates the possibility of the development of a high-resolution temperature measurement system in the near-field.

6 Conclusion

We have demonstrated the utility of near-field fluorescence as a temperature measurement technique at the nanoscale. Mono-reactive Cy3 dye was selected as a fluorophore, and preliminary measurements were carried out to investigate the fluorescent emission spectrum and temperature dependence near room temperature under the fluorescent microscope. In order to discuss the validity of the positioning and detection system of Fluor-NOTN, we have fabricated a metallic wire heater sample of 500 nm in width and 100 nm in thickness, and measured its Cy3 modified surface topography, fluorescent distribution, and detected localized temperature gradient.

In this article, the localized temperature gradient within a submicron distance from the wire heater edge is detected by near-field fluorescence. The result indicates successful development of a temperature-responsive measurement system using a near-field optical fiber and mono-layered Cy3 fluorophore.

Acknowledgments This research was partially supported by the Ministry of Education, Culture, Sports, Science and Technology, Grant-in-Aid for No. 16206023 (A)(2), Charitable trust Nissin-Sugar Manufacturing and the 21st Century Center of Excellence for “System Design: Paradigm Shift from Intelligence to Life.”

References

1. P. Avouris, J. Appenzeller, R. Martel, S.J. Wind, Proc. IEEE **91**, 1772 (2003)
2. M. Babincova, P. Sourivong, D. Leszczynska, P. Babinsec, Phys. Medica **19**, 213 (2003)
3. D.G. Cahill, W.K. Ford, K.E. Goodson, G.D. Mahan, A. Majumdar, H.J. Maris, R. Merlin, S.R. Phillpot, J. Appl. Phys. **93**, 793 (2003)
4. E. Pop, K.E. Goodson, Proc. Intersociety Conf. **1**, 1 (2004)
5. L. Shi, A. Majumdar, J. Heat Transfer **124**, 329 (2002)
6. Y. Gao, Y. Bando, Z. Liu, D. Goldberg, Appl. Phys. Lett. **83**, 2913 (2003)

7. D. Ross, M. Gaitan, L.E. Locascio Anal. Chem. **73**, 4117 (2001)
8. E.V. Keuren, D. Littlejohn, W. Schrof, J. Phys. D: Appl. Phys. **37**, 2938 (2003)
9. M. Kobayashi, Y. Horiguchi, Y. Taguchi, T. Saiki, Y. Nagasaka, Proc. Eur. Conf. Thermophys. Props. (2005)
10. Y. Amao, I. Okura, Analusis **28**, 847 (2000)
11. K. Kaneto, H. Hasegawa, Proc. SPIE—The Int. Soc. Opt. Eng. **3142**, 216 (1997)
12. M. Ohtsu, *Near-field Nano/Atom Optics and Technology* (Springer, Hong Kong, 1998)
13. J.R. Lakowicz, *Principles of Fluorescence Spectroscopy*, 2nd edn. (Kluwer Academic/Plenum Pubs, New York, 1999), pp. 10–11
14. A. Bejan, *Heat Transfer* (John Wiley & Sons Inc., New York 1993), pp. 120–125
15. B.G. Moreira, Y. You, M.A. Behlke, R. Owczarzy, Biochem. Bioph. Res. Co. **327**, 473 (2005)
16. P. Constantinou, T. Nicklee, D.W. Hedley, S. Damaskinos, B.C. Wilson, IEEE J. Selected Topics Quant. Elect. **11**, 766 (2005)
17. A. Lakkaraju, Y.E. Rahman, J.M. Dubinsky, J. Bio. Chem. **277**, 15085 (2002)